Myeloid dendritic cells repress human cytomegalovirus gene expression and spread by releasing interferon-unrelated soluble antiviral factors

Bahram Kasmapour,[1] Tobias Kubsch,[1] Ulfert Rand,[1] Britta Eiz-Vesper,[2] Martin Messerle ,[3] Florian W. R. Vondran,[4,6] Bettina Wiegmann,[5] Axel Haverich,[5] Luka Cicin-Sain[1,3,6]#

Immune Ageing and Chronic Infections Group IMCI, Helmholtz Centre for Infection research HZI, Braunschweig, Germany[1]; Institute for Transfusion Medicine, Hannover Medical School MHH Hannover, Germany[2]; Institute of Virology, Hannover Medical School MHH Hannover, Germany[3]; Department of General, Visceral and Transplant Surgery, Hannover Medical School MHH, Hannover, Germany[4]; Department of Cardiothoracic, Transplantation and Vascular Surgery, Hannover Medical School MHH, Hannover, Germany[5]; German Centre for Infection Research (DZIF), Location Hannover-Braunschweig[6]

Running Head: human mo-DCs repress HCMV gene expression

#Address correspondence to Luka Cicin-Sain, lcs09@helmholtz-hzi.de

Abstract word count: 222, Text word count: 6150

Abstract

Cytomegalovirus (CMV) is a beta-herpesvirus that latently infects most adult humans worldwide and is a major cause of morbidity and mortality in immunocompromised hosts. Latent human CMV (HCMV) is believed to reside in precursors of myeloid-lineage, leukocytes and monocytes, which give raise to macrophages and dendritic cells. We report here that human monocyte derived DCs (mo-DC) suppress HCMV infection in coculture with infected fibroblasts target cells in an effector-to-target-ratio dependent manner. Intriguingly, optimal activation of mo-DC was achieved in coculture conditions, not by their direct infection with HCMV, implying that mo-DC may recognize unique molecular patterns on, or within, infected fibroblasts. We show that HCMV is controlled by secreted factors that act by priming defenses in target cells rather than by direct viral neutralization, but we excluded a role for IFNs in this control. The expression of lytic viral genes in infected cells and the progression of infection were significantly slowed down, but this effect was reversible, indicating that the control of infection depended on the transient induction of antiviral effector molecules in target cells. Using immediate-early or late-phase reporter HCMVs, we show that soluble factors secreted in the cocultures suppress HCMV replication at both stages of the infection and that their antiviral effect is robust and comparable in numerous batches of mo-DCs as well as in primary fibroblasts and stromal cells.

Importance

Human cytomegalovirus is a widespread opportunistic pathogen that can cause severe disease and complications in vulnerable individuals. This includes newborn children, HIV AIDS patients or transplant recipients. Although the majority of healthy humans carry this virus throughout their lives without symptoms, it is not exactly clear which tissues in the

body are the main reservoirs of latent virus infection, or how the delicate balance between the virus and the immune system is maintained over the individual's lifetime. Here for the first time, we provide evidence for a novel mechanism of direct virus control by a subset of human innate immune cells called Dendritic Cells, which are regarded as a major site of virus latency and reactivation. Our findings may have important implications in HCMV disease prevention as well as development of novel therapeutic approaches.

Introduction

Human cytomegalovirus (HCMV) causes a subclinical primary infections in approximately 50 to 100 percent of healthy individuals, depending on geographical and socio-economical differences of populations (1). Primary infection is followed by lifelong latent infection, which typically remains asymptomatic. HCMV infection is the most common cause of congenital infections, which may result in birth defects, and a major risk for complications in immune-suppressed and -compromised individuals (2-4). There is no vaccine available against HCMV. Therefore, the immune response and therapeutic strategies against this virus remain subjects of intense studies.

HCMV infection elicits a strong immune response (5). The role of natural killer (NK) and T cells in controlling the primary infection as well as preventing reactivation from latency has been well-documented in animal models of cytomegalovirus infection (6, 7). The role of dendritic cells (DC) remains somewhat less clear, partly because HCMV replicates in some DC subsets. The major DC subsets in humans include the myeloid or classical (cDC), the plasmacytoid (pDC) and the monocyte-related (mDCs), where the last type includes the inflammatory CD1c+, CD16- DCs (8). HCMV can initiate a replicative infection in the *in vitro* generated monocyte derived DCs (mo-DCs) (9-12) or in the *ex vivo* harvested circulating

mDCs that closely resemble the phenotype of mo-DCs (13). HCMV *in vitro* infection triggers interferon and other cytokine responses in mo-DC (14) in a cGAS dependent manner (15), and this may recruit other immune subsets to the site of infection and coordinate the immune response. On the other hand, HCMV downregulates HLA I expression and upregulates Fas ligand and TRAIL in infected DCs, protecting them from cytolytic cells and inducing apoptosis in activated T cells interfacing with them (16). Additionally, HCMV expresses an IL-10 homolog in infected cells (17), which suppresses IFN-α/β production in nearby pDC (18, 19). Taken together, numerous DC subsets interact with HCMV in a pleiotropic manner (20). They are essential for inducing the antiviral NK and T cell responses, but also a target of HCMV infection and immune evasion (21). However, DC responses to HCMV infection have so far been studied in DC monocultures, probably due to their permissiveness for HCMV and the assumption that mo-DC are triggered by direct viral infection. Notably, we found recently that murine cDCs release antiviral factors that control mouse CMV in co-cultured fibroblasts or endothelial cells (22).

CMVs have coevolved with the host species and are strictly specific for the respective host cells, impairing our ability to study HCMV biology by *in vivo* infection models. Nevertheless, there are significant similarities between CMV of different species at the level of viral genes and their functions (23-25), and the murine CMV (MCMV) is widely used as model of virus-host *in vivo* interactions. Murine pDC are the major source of type I interferon response to MCMV infection (26), yet do not support a replicative infection (27). Murine cDCs on the other hand can be infected with MCMV, but produce lower amounts of type I IFNs (20, 28). *In vivo* experiments have shown that DCs contribute to the control of CMV infection by indirect mechanisms inducing antiviral responses of NK and T cells (27, 29-31). More recently, we showed direct repression of MCMV infection and spread by bone marrow

derived DCs (mDC) (22) in coculture with infected endothelial and fibroblastic cells. The antiviral function was mediated by type 1 IFN secretion as well as other yet unidentified soluble antiviral factors (22).

We hypothesized that a similar antiviral function may be exerted by HCMV and therefore, studied the ability of human mo-DCs to control HCMV replication in human endothelial and fibroblastic cells. Here, we show a robust dose-dependent control of HCMV replication in fibroblasts cocultured with mo-DCs, mediated by soluble factors released into the supernatant. The antiviral factors stimulated the innate antiviral defenses of the target cells and repressed the expression of immediate early as well as late HCMV genes, thereby slowing the progression of the infection in a reversible manner. In contrast to the previously reported results in the murine system, this was not dependent on signaling via Interferon-alpha/beta receptor (IFNAR). Finally, we show that only cocultures of infected fibroblasts and mo-DC induced the supernatants from displayed antiviral properties, whereas supernatants from monocultures of HCMV-infected mo-DC were not protective against HCMV spread in human cell lines or in primary human fibroblasts and stromal cell cultures.

Results

Human mo-DCs suppress spread of HCMV infection in cocultured human fibroblasts

To test the ability of human DCs in controlling HCMV replication in coculture with virus-infected target cells, we generated mo-DC populations by differentiating CD14+ blood monocytes using a conventional protocol (32). We infected MRC-5 fibroblasts with the dual late-gene reporter virus, TB40/E-UL32GFP/UL100mCherry (HCMV^{dLr}) (33) at a multiplicity of infection (MOI) of 0.0125 plaque forming units (PFU) per target cell, which enabled reliable counting of infected cell in a 96-well plate format. After two hours of infection, the virus suspension was removed from cells and mo-DCs (effector cells) were added to the infected MRC-5 cells (target cells) at effector to target (E:T) ratios between 5:1 to 1:1 (**Fig. 1A,** experimental scheme in Fig. S1A). At 5-6 days post infection (dpi), the infected GFP and mCherry expressing MRC-5 cells were identified by epifluorescence microscopy and counted in each well (**Fig. 1A**). We observed a dose-dependent control of infection that reached statistical significance at E:T 2:1, where we observed about a 75% reduction in number of infected cells (**Fig. 1A**). To facilitate a faster work-flow, we adopted a rapid mo-DC generation protocol, which allowed to differentiate and mature mo-DCs during 4, instead of 9 days (34). We validated the functional similarity of rapidly generated mo-DCs to the conventionally generated ones by testing virus control in identical settings and included an extended range of E:T ratios (**Fig. 1B**). We observed the same dose-dependent control starting at E:T ratios 1:1 to 2:1, and an almost complete absence of infected cells at ratios 10:1 and 15:1. The mo-DCs were generated from PBMCs from several CMV seronegative donors, but despite some variation in potency among different donors (data not shown), almost all mo-DCs batches showed the same robust trend of dose-dependent control. To

see if this repression correlated with reduction of lytic replication of the virus, cells were infected and cocultured with mo-DC at E:Ts of 20:1, 10:1 and 4:1. At 14 dpi, infectious virus titers in the supernatants were compared to control wells infected in absence of mo-DC by plaque assay, where we observed significant reductions in the presence of mo-DC (**Fig. 1C**).

To define the kinetics of HCMV spread in the presence of mo-DCs, we monitored HCMV^{dLr}-infected cocultures of MRC-5 and mo-DCs at E:T of 10:1 over 15 days and compared them to control conditions without mo-DCs. To allow for dynamic quantification of infected cells up to 15 dpi, cells were infected with 45 PFU/well (MOI=0.0015) and counted at 6, 9, 12 and 15 dpi. We observed major differences at every time point, with less than 10 infected cells per well detectable at all times (**Fig. 1D,** blue squares), whereas the numbers expanded rapidly in control wells lacking mo-DCs (**Fig. 1D,** black circles). To assess if the antiviral effect is reversible, mo-DCs along with the supernatant content of the well were removed and replaced with fresh medium at 6 dpi and infection was monitored until dpi 15 (**Fig. 1D,** red triangles). The number of infected cells increased at a higher rate than in wells where mo-DCs were left in coculture. To determine if infection can be fully eliminated by the mo-DCs, or if virus replication may restart even after the virus was entirely contained, cells were infected with the HCMV^{dLr} at a much lower MOI of 0.0002 (6 PFUs/well), at which it was reliably possible to detect at least one infected cell per well in control conditions. Six days later, we surveyed all 12 replicates wells for the presence of any infected cell (i.e. positive well). While almost all control wells contained an infected cell and were therefore positive (**Fig. 1E,** black), approximately 8 out of 12 mo-DC containing wells remained negative. Mo-DCs were removed (red triangles) or not (blue squares) at 6 dpi and infection was monitored for an additional 15 days (**Fig. 1E**). By 21 dpi, almost all previously negative wells from which

153 the mo-DCs were removed became positive, whereas this was the case in only a few mo-DC
154 containing wells (blue squares).

155 Therefore, monocyte derived human DCs potently suppressed the spread of HCMV infection
156 in cocultured human fibroblasts. This block occurred in a ratio-dependent manner and
157 required continuous surveillance, but was independent of the mo-DC generation protocol.
158 Consequently, the rapid mo-DC generation protocol was used in subsequent experiments.

159 ## Mo-DCs suppress the spread of HCMV and repress expression of the major
160 ## immediate early genes ie1/2

161 While the coculture with mo-DC reversibly impaired HCMV spread, it remained unclear
162 whether the effects occurred at early or at late stages of the infection cycle. Namely, as the
163 fluorescent reporter genes in HCMV^{dLr} are expressed by late viral promoters, their
164 expression would be affected by blocks in both the early, and the late stage. Thus, we
165 generated a novel immediate-early reporter virus TB40/E-UL122/123mNeonGreen (HCMV^{IEr})
166 expressing the bright mNeonGreen fluorescence protein (35) under the control of the
167 endogenous HCMV major immediate-early promoter and in equimolar ratio to the total
168 products of ie1 and ie2 genes (**Fig. S2A**). We infected MRC-5 cells with 150 PFU of HCMV^{IEr}
169 (MOI=0.005), cocultured them with mo-DCs at various ratios (**Fig. 2**) and counted the
170 number of infection foci per well at 3 dpi (**Fig. 2A**). As observed with the HCMV^{dLr}, mo-DCs
171 suppressed the spread of infection in a E:T ratio-dependent manner, yet a complete
172 abrogation of infection could not be achieved even at high ratios. In fact, single infected cells
173 kept appearing over time and the size of infection foci increased even under high E:T ratios.
174 Nevertheless, the progression of infection was significantly slowed down in the presence of
175 mo-DCs, resulting in a striking contrast between high and low ratio conditions (15:1 vs 4:1)
176 and w/o mo-DC controls at dpi 8 (**Fig. 2B**) or 23 (**Fig. 2C**). To define if mo-DC may entirely

177 block HCMV spread in ideal conditions, we monitored the mNeonGreen signal upon
178 infection at very low dose of HCMV^{IEr} (6 PFU/well = MOI 0.0002), using the same conditions
179 as applied before in the experiment depicted in **Fig. 1E**. Virtually all control wells (black
180 circles) were positive at dpi 6 (**Fig. 2D**), while approximately half of the 12 wells remained
181 negative in presence of mo-DCs (blue squares and red triangles). Removal of mo-DC at 6 dpi
182 led to a spike in number of positive wells already 3 days later (red triangles), and by 15 dpi,
183 all wells from which mo-DCs were removed were positive. Unlike in the experiment shown in
184 Fig. 1E, however, the number of positive wells increased even in the continuous presence of
185 mo-DC in coculture (blue squares), albeit at a slower pace, yet by the end of the experiment,
186 almost all wells from all conditions were positive (**Fig. 2D**).

187 We therefore conclude that mo-DCs may repress, but not fully block, the expression of
188 HCMV lytic genes. Since the block was more pronounced at late stages (Fig. 1) than at the
189 immediate-early one (Fig. 2), our data indicated that the antiviral effects might act at the
190 level of both phases and accumulate with the progression of the infection

191 **Antiviral function of activated mo-DCs is mediated via soluble factors that delay**
192 **and repress IE gene expression**

193 We hypothesized that mo-DCs may suppress viral replication by releasing soluble antiviral
194 factors. In that case, viral gene expression would be repressed by conditioned supernatant
195 (SN°) from mo-DC cocultures. To test this, we harvested supernatant of mo-DCs coculture
196 with infected MRC-5 at 6-8 dpi and filtered it through 0.1 µm pore-size filters to remove cells
197 and virus particles (**Fig. S1B**). We followed the early dynamics of HCMV gene expression in
198 real-time by live cell imaging. The infection of MRC-5 fibroblasts with HCMV^{IEr} was
199 synchronized by restricting the infection to a 10-minute window (36). SN° was added
200 immediately upon virus removal and the reporter signal was dynamically monitored and

quantified. In control condition, the IE-reporter signal became detectable at approximately 3 hpi (**Fig. 3C**) and steadily increased as the infection progressed (**Fig. 3A, B,** blue). In SN° treated cells however, the onset of the signal was significantly delayed, starting at approximately 5 hpi (**Fig. 3B, 3C,** red) and increased at a reduced rate (**Fig. 3A**). The intensity of the reporter signal, and therefore IE gene expression, increased strikingly faster in untreated control cells (**Fig. 3A** blue) and this correlated with prominent changes in cell morphology as well as disruption of the cell monolayer (**Fig. 3D,** second row; see also **Movie S1)**.

Antiviral function of mo-DCs is independent of type I interferon

DC are known to secrete interferon (IFN) beta and alpha in response to CMV infection (37), and thus we considered it likely that type I IFNs are the soluble factors repressing HCMV replication in our system. Therefore, we measured the available IFN-β in the mo-DC coculture SN by high-sensitivity ELISA (**Fig. 4A & Fig. S3A**). The concentration of the available IFN-β was elevated in infected cocultures over MRC-5 monocultures, but reached concentrations of only 2-8 U/mL at E:T 20:1 and E:T 4:1 ratios. We considered the possibility that the released type I IFNs are immediately bound to receptors on target cells, and thus measured IFN levels in the presence of α-IFNAR2, that blocks attachment of IFN-β to subunit 2 of the heterodimeric common type I IFN receptor IFNAR (38). In presence of α-IFNAR2, the IFN-β concentration was significantly higher and reached approximately 30-50 U/mL (**Fig. 4A**). This argued that activated mo-DCs generate significant amounts of IFN-β and that IFN-β is sequestered from SN by the IFNAR in cocultures. We next tested the effect of the concentration of IFN-β added after infection on the control of HCMV in MRC-5s. We observed that IFN-β concentrations up to 30-50 U/mL correlated with improved protective effect at all MOIs tested, but further increases were ineffective (**Fig. S3B**).

225 To test if the mo-DC suppress HCMV infection by releasing type-I IFN, we used the α-IFNAR2
226 antibody to block downstream IFNAR signaling (39). Cocultures of mo-DCs and infected
227 MRC-5 at E:Ts of 20:1, 10;1 and 4:1 were treated with 10 µg/mL α-IFNAR2 starting at 24 h
228 before infection and maintained for the duration of the experiment (**Fig. 4B**). We observed
229 the E:T ratio-dependent reduction of virus titers, and blocking of IFN type I signaling did not
230 lead to the rescue of virus titers relative to untreated wells (**Fig. 4B**). If anything, IFNAR
231 blocking consistently decreased the viral titer in presence of mo-DCs, although this effect
232 was not statistically significant (**Fig. 4B).** We considered the possibility that α-IFNAR2 effects
233 may be manifest at gene expression level rather than at the PFU level. Therefore, we
234 measured mNeonGreen expression upon infection with HCMV^{IEr} yet in the presence of mo-
235 DC and α-IFNAR2. We observed no increase in the number of infected cells over the control
236 cocultures lacking α-IFNAR2 (**Fig. 4C**) and they were not enlarged in the presence of α-
237 IFNAR2 (**Fig. 4D**). In fact, the foci appeared smaller in α-IFNAR2 presence, matching the PFU
238 results (**Fig. 4B**). In sum, the evidence argued against a major role for type I IFN in the
239 observed antiviral effect of mo-DCs.

240 We considered the possibility that the IFNAR-2 blocking antibody might not be sufficiently
241 efficient at blocking antiviral IFNAR effects in our assays. Therefore, we tested HCMV^{IEr}
242 replication in MRC-5 fibroblasts in presence of IFN-β and IFNAR2 blocking antibodies (**Fig.**
243 **S4A**). While IFN-β fully abrogated infectious virus titer if added before infection and
244 significantly reduced it if added immediately post infection, IFNAR2 blocking antibodies
245 dampened this effect, increasing the virus titer (**Fig. S4B**). We also tested the effect of
246 various concentrations and timings for α-IFNAR2 as well as IFN-β treatments (**Fig. S4C**). Data
247 showed that α-IFNAR2 could effectively block IFNAR signaling and thus block the antiviral

effect of IFN-β that was added to infected cells just after the infection at concentrations up to 500 U/mL (**Fig. S4C**).

Since mo-DCs produced comparable levels of IFN-β at E:T 4:1 and 20:1 ratios (**Fig. 4A**) at which the antiviral effects were not identical (**Fig. 2A**), and blocking IFNAR did not diminish the antiviral effect of mo-DCs (**Fig. 4B-D**), our data argued that IFN signaling did not play a major role in the control of HCMV by mo-DCs.

Antiviral factors from mo-DCs stimulate antiviral defenses of target cells

The antiviral action of mo-DCs was mediated by soluble factors beyond IFN type I. We considered the possibility that the antiviral activity may occur by factors directly interacting with viral particles (40), viral gene product (41), or by factors that elicit signaling pathways and activate cellular antiviral defenses of the target cells.

We tested these scenarios by additionally treating MRC-5 with the antiviral supernatant for 24 h before the infection, or at the time of infection, and comparing these cells to those where SN° was added just after HCMV^{IEr} infection (**Fig. 5A**). We measured the rate of infection and the mNeonGreen signal by flow-cytometry (**Fig. 5B**). While the frequency of infected cells was reduced in all SN°-treated groups, pre-treatment of cells with the SN° lead to the most effective control of infection (**Fig. 5C, S5B**). Adding SN° only after infection was the least protective and adding the SN° at the time of infection resulted in an intermediate antiviral effect. Likewise, SN° pretreatment reduced the reporter mean fluorescence signal intensity (MFI) more efficiently than SN° added at the time of infection, or only after infection (**Fig. 5D**). Suppression of infection did not correlate significantly with loss of cell viability (**Fig. S5A, 2B-C)**. Therefore, our data argued that the antiviral SN acts by inducing non-cytotoxic antiviral signaling pathways in target cells.

Mo-DCs are activated by contact with infected MRC-5 cells, but not by direct infection

It remained unclear if the antiviral function of mo-DC was stimulated by simple contact with uninfected MRC-5 cells, by direct virus infection, or by contact with infected MRC-5 cells. Therefore, we compared the effect of conditioned SN from (i) infected mo-DC/MRC-5 cocultures, (ii) uninfected cocultures of DCs and MRC-5 cells or (iii) mo-DCs infected with HCMV in absence of MRC-5 cells. Conditioned SN was added to MRC-5 cells infected with the dual late reporter HCMV^{dLr} and their effect defined by comparing the spread of infection at dpi 5-6. Only the SNs from infected mo-DC/MRC-5 cocultures effectively suppressed HCMV^{dLr} spread (**Fig. 6A&B**), whereas SN from uninfected cocultures did not. Even more intriguingly, SN from mo-DCs directly infected with HCMV, in the absence of MRC-5 cells, did not inhibit virus spread (**Fig. 6B**). We repeated the assay using the immediate-early HCMV^{IEr} reporter virus (**Fig. 6C&D**). As in the case of the late reporter, only the SN from infected cocultures reduced HCMV^{IEr} spread (**Fig. 6C, 6D**), and it was irrelevant if HCMV^{IEr} or HCMV^{dLr} was used for the infection of the primary coculture. Likewise, SN from DCs infected in absence of MRC-5 or from uninfected DC-MRC-5 cocultures showed no antiviral effect. Finally, we tested the supernatants from different co-culture and/or infection conditions for multiple IFNs, including IFN-α2, -β, -γ, -λ1 or λ2/3. While we observed a clear induction of all IFN responses in HCMV infected DC monocultures, none of them was induced in the case of the antiviral SN° derived from infected MRC-5+mo-DC co-cultures (**Fig. 6E**).

Taken together, these data indicated that mo-DC secreted antiviral factors repressing HCMV IE and late gene expression are independent of major type I-III interferons and are only induced by the interaction of mo-DC with infected MRC-5 cells, arguing that mo-DC possess sensors that recognize infected cells and trigger their activation.

295 ## Antiviral function of mo-DCs is maintained in primary target cells

296 To test if mo-DC antiviral activity is restricted to the control of HCMV in the fibroblastic cell
297 line MRC-5, or if it acts broadly in primary HCMV permissive cells of different origins, we
298 isolated primary stromal cells from human lung and liver tissue and used them in coculture
299 experiments. These cells were primarily composed of fibroblastic and endothelial cell types,
300 and were compared to primary human foreskin fibroblasts infected with HCMV^{IEr} and
301 cocultured with mo-DC (**Fig. 7A).** mo-DCs suppressed the spread of infection in an E:T ratio
302 dependent manner in most primary cell cultures, with robust antiviral effect observed is
303 some (**Fig. 7A**, Lung#38), although not in all lines (**Fig. 7A**, Lung#78). Antiviral SN from
304 infected mo-DC/MRC-5 cocultures had a similar effect on HCMV^{IEr}-infection in primary cell
305 cultures (**Fig. 7B**). Therefore, the antiviral effect of mo-DCs was not exclusive to the MRC-5
306 cell line and is likely to act on a wide variety of cell types. Taken together, our data show that
307 soluble factors secreted from human mo-DCs are able to repress HCMV gene expression and
308 suppress the spread of infection in a variety of target cells independently of IFN-β.

309 ## Discussion

310 Numerous studies have demonstrated the ability of CMV to infect and establish latency in
311 monocytes and DCs derived from them (21, 42-45), but these studies were customarily
312 focused on the study of mo-DC behavior in monocultures. We showed recently a role for DCs
313 in controlling CMV infection in nearby cells in a murine model, where *in vitro* infected
314 fibroblasts or endothelial cells were cocultured with mDC (22). We expand on the findings
315 from that report and show that human mo-DC are activated by HCMV infected fibroblasts in
316 a manner that functionally differs from direct infection of mo-DC in monocultures. While the
317 identity of this trigger at the molecular level goes beyond the scope of this study, its broader

318 implication is that in addition to recognizing pathogen-associated molecular patterns, mo-
319 DCs may also detect nearby infected cells and likely engage in receptor/ligand interactions
320 with them. In this report, we provide evidence of this novel immune sensing mechanism.

321 We partly identified the mechanism of antiviral action of mo-DC; we demonstrate that
322 HCMV is contained by soluble factors released in mo-DC/fibroblast cocultures, and that
323 these factors already act during, or before immediate-early gene expression. While viral
324 repression was even stronger at later stages of the viral replication cycle, one needs to
325 consider that any cumulative antiviral effects would result in a more profound repression of
326 the virus at later stages. Importantly, the antiviral effects were stronger if the target cells
327 were pretreated with the conditioned supernatants, arguing against direct virus inactivation
328 (40). Therefore, our data may be consistent with a model where factors released by mo-DCs
329 induce antiviral effector pathways in the target cells.

330 Based on our data from the murine model, we considered type I IFN signaling to be a likely
331 candidate for driving the antiviral effect, but assays with the IFNAR-blocking antibody argue
332 against this scenario. On the other hand, data from the murine system did not exclude the
333 possibility that IFN signaling requires synergizing with additional factors to control MCMV
334 (22). Therefore, we cannot exclude the possibility that the antiviral action of human mo-DCs
335 partially overlaps with the mechanisms in murine cocultures. Both murine and human DCs
336 blocked viral gene expression at the immediate early stage, and viral gene expression was
337 reconstituted upon mo-DC removal from cocultures, resembling reactivation phenotypes in
338 HCMV models of *in vitro* latency (43, 46, 47). Since the balance of virus latency appears to
339 hinge on cell-signaling (48) and may be influenced via cellular inflammatory cytokines (42,
340 49) our data raise the possibility that factors released by myeloid cells, or by their
341 precursors, may actively regulate viral gene expression and replication, balancing HCMV

342 latency and reactivation. Considering that all currently studied *in vitro* models of HCMV
343 latency are based on the infection of monocytes or their precursors, our data raise the
344 intriguing possibility that at least part of this phenomenon is due to autocrine or paracrine
345 factors released by myeloid cells (49).

346 We used a novel HCMV reporter virus in this study, in which a fluorescence reporter gene
347 was expressed by the endogenous major immediate-early promoter. Live-cell imaging of
348 cells infected with this virus have allowed us to show that mo-DCs delay immediate-early
349 gene expression, although they do not entirely abrogate its expression. Future research will
350 focus on the identification of the soluble factors critical for HCMV control at this stage, in
351 order to appraise the feasibility of their utilization for treatment of HCMV infection and
352 disease. By developing the *in vitro* model of mo-DC/fibroblast coculture, we have opened
353 the doors towards such approaches.

354

355 ## Materials and methods

356 ### Cells

357 Human embryonic lung fibroblast MRC-5 (ATCC® CCL171) were maintained in Eagle's
358 Minimum Essential Medium (EMEM, Sigma-Aldrich, #M5650) supplemented with 10% FCS,
359 1% Sodium Pyruvate, 1% Penicillin/ Streptomycin and incubated at 37°C with 5% CO_2.
360 Human monocyte derived DCs (mo-DC) were generated and maintained in RPMI 1640
361 medium (Sigma-Aldrich) supplemented with 10% FSC and 1% Penicillin/ Streptomycin and
362 incubated at 37°C with 5% CO_2. Human primary stromal liver and lung cells were isolated
363 from donated liver tissue biopsy samples and explanted lung tissue of transplant recipients
364 from the Hanover Medical School, as described elsewhere (50, 51) and maintained in EGM-
365 2MV primary endothelial medium (Lonza). Primary human foreskin fibroblasts were
366 cultivated in high glucose Dulbecco's Modified Eagle's Medium (DMEM, Sigma-Aldrich,
367 #D5796) supplemented with 10% FSC and 1% Penicillin/ Streptomycin and incubated at 37°C
368 with 5% CO_2.

369 ### Generation of human monocyte-derived DCs

370 PBMCs were isolated from leukoreduction system (LRS) filter chambers used in apheresis
371 machines of the Institute for Transfusion Medicine of the Hannover Medical School as
372 described before (52) within 18 hours after the donation by healthy individuals using
373 Lymphoprep (Stemcell technologies, Canada) density gradient centrifugation (53).
374 *Conventional mo-DC generation protocol:* As described previously (32), monocytes were
375 separated form rest of PBMCs via two subsequent rounds of plastic adherence in serum free
376 RPMI (54) or magnetically sorted (MACS) using α-CD14 microbeads (human CD14+
377 Microbeads and AutoMACS Pro separator Miltenyi Biotec, Germany) and cultivated at $2x10^6$
378 cells/mL in full RPMI with 800 U/mL GM-CSF (Peprotech, USA) and 500 U/mL IL-4

(Peprotech, USA) for five days, after which they were transferred to full fresh RPMI containing GM-CSF, IL-4 and 100U/mL TNF-α (R&D Systems, USA) for an additional 3-5 days of maturation. Mature conventionally generated mo-DCs were then thoroughly washed and pelleted three times in PBS and used in experiments within 6 hours. *Rapid generation protocol:* as previously shown (34, 55, 56), MACS sorted CD14+ monocytes were cultivated at 1-2x10^6 cells/mL in full RPMI in the presence of differentiation cocktail containing 200-500 U/mL GM-CSF, 50-200 U/mL IL-4 and 1,000 U/mL IFN-β for 36-48 hours. Thereupon, 200 U/mL TNF-α (Peprotech, USA), 5,000-1,000 U/mL IL-1β (Peprotech, USA) and 1µg/mL prostaglandin E2 (PGE2, Biolegend, Germany) were added for an additional 2-3 days to induce DC maturation.

Viruses

In the dual reporter HCMV strain TB40/E-UL32-GFP/UL100-mCherry, EGFP and mCherry are fused to the C-terminus of the late phase capsid-associated tegument protein pUL32 (pp150) and the envelope glycoprotein M (UL100) respectively, expressing readily detectable green and red fluorescence signals in lytically infected host cells as described elsewhere (33). Reporter HCMV strain HCMV TB40/E-UL122/123-mNeonGreen was generated using e*n passant* BAC mutagenesis (57) on a TB40/E-BAC background (genebank#EF999921) as described elsewhere (58), with the difference that the US region of the BAC is inverted relative to the original BAC. The mNeonGreen (mNG) gene, coding a novel bright green fluorescent protein (Allele Biotech, USA) (35), linked to the P2A peptide (59) was inserted before the start codon of UL122/123 exon 2 (**Fig. S2A**). Endogenous HCMV major immediate-early (MIE) promoter drives mNG-P2A expression in an equimolar ratio with the products of MIE genes UL123 (IE1) and UL122 (IE2). Ribosomal skipping between glycine 21 and proline 22 of P2A peptide causes efficient cleavage at this position, separating mNG with

a 23 amino acid long residue, 2 linker AAs plus 21 of the P2A, on its C-terminus, while leaving one proline from P2A at the N-terminus of the exon 2 of MIE gene products, effectively minimizing risk of interference with function of viral proteins compared to a fusion protein approach. The reporter insertion and final BAC sequence were confirmed by Sanger sequencing. The reporter virus has identical growth kinetics with its parental virus (**Fig. S2B)**.

Coculture with the monocyte derived dendritic cells, mo-DCs

Immediately after virus suspension was removed, monocyte derived dendritic cells, harvested from maturation within 6 hours of the start of the experiment, were added to infected target cells at defined effector to target (E:T) ratios in 200 µL full medium (based on target cells) per well in 3-12 well replicates. A schematic outline is depicted in **Fig. S1A**.

Generation and processing of antiviral coculture supernatant

Mo-DCs were added to uninfected or HCMV infected (MOI 0.01, 2 h) MRC-5 at E:T of 10:1, or mo-DCs were left uninfected or infected for 2 h with HCMV at MOI 1.0, in wells of a 6-well plate or 3.5 cm culture dish, containing 5 mL full RPMI medium. After 6-8 days, the well content was collected and centrifuged for 5 minutes at 700 g at 4°C to remove cells and debris, filtered through a 0.1µm-pore size syringe mounted filter, aliquoted and frozen at -20°C until use. A schematic outline is depicted in **Fig. S1B**.

Virus titration

The titer of cell-free virus in well supernatant was quantified by plaque assay. At the readout time point, SN was removed and frozen at -80°C before use. 100 µL of SN was serially diluted in full EMEM and added to 30,000 fresh MRC-5 seeded one day in advance for two hours of incubation. Virus suspension was removed and cells were overlaid with EMEM containing 5%

carboxymethylcellulose. After 5-8 days of incubation, virus plaques were counted and the virus titer is reported as plaque forming units (PFU) per milliliter of SN.

Infection and quantification by microscopy

Human embryonic fibroblast-like cell line MRC-5 or foreskin fibroblasts HFF were seeded at 25,000 cells/well in flat bottom 96 well plates one day before infection. Human primary stromal cells from lung and liver were seeded in numbers to reach 30,000 on the day of infection, on 0.2% gelatin (in PBS solution) coated plates. For infection, virus was added in 100 µL suspension in defined multiplicity of infection (MOI) and incubated at 37°C for two hours, before the virus suspension was removed. When TB40E-UL32GFP-UL100mCherry dual late-gene reporter virus (HCMV^{dLr}) was used, infected single cells expressing both the green EGFP and the red mCherry fluorescence signals were counted at 5-6 dpi unless stated otherwise. When the TB40E-UL122/123-mNeonGreen immediate early reporter virus (HCMV^{IEr}) was used, mNeonGreen expressing infection foci (group of several infected cells that do not yet show clearly observable CPE) were visible already by day 2. The foci were quantified at day 2-3 before merging of growing adjacent foci or spread of secondary infection would affect the readout (**Fig. S1A)**. Alternatively, a centrifugal enhancement protocol of infection was used when synchronous infection of target cells was required. Virus suspension in 100µL per well was centrifuged at 2000 rpm, for 10 min at room temperature, essentially as described elsewhere (36). This protocol increased the rate of infection by a factor of 3-5 compared to the 2 h incubation method and therefore MOIs for these was based on centrifugally enhanced virus titration.

Live cell imaging and quantification

MRC-5 fibroblasts were seeded at 75,000 cells/chamber on glass bottom live cells imaging dishes (Hi-Q^4, ibidi) and infected at an MOI of 0.035 with the centrifugal method, followed

Journal of Virology

by removal of the virus suspension. A BioStation IM-Q live-cell screening system (Nikon, Japan) with a complete environmental incubation system was used to follow the infection for up to 8 days. Images were acquired from up to 24 fields per condition at 20X magnification, 1024*940 pixels in bright field, GFP and TexasRed channels when applicable, at 12% illumination intensity, 500 ms exposure and 5.6 gain settings for fluorescence channels with acquisition rates one image per every 20 to 60 min. Time series stacks for all fields were analyzed automatically using an in-house created Fiji (ImageJ) (60) macro (**supplementary materials & methods and Fig. S6**). Briefly, the bright IE-mNeonGreen signal was used to detect infected cells and then to measure and reports the mean fluorescence signal intensity for infected cells and the background in each frame, in the GFP (for mNeonGreen) channel of the BioStation IM-Q. Mean signal from all cells in a frame was divided by the mean background signal (i.e. signal ratio) in order to compensate random signal fluctuations, as well as field-to-field and experiment-to-experiment variations (e.g. see **Fig. 5G** & **Movie S1**), and was plotted in Graph Pad Prism. Onset time was defined as the time point of the first frame after which the signal ratio steadily increased in every subsequent frame (i.e. point of true deviation from asymptote) and was analyzed manually.

Blocking of type I interferon signaling

Antibody against the Human Interferon (alpha, beta and omega) Receptor 2 (IFNAR2, PBL Assay Science, USA #21385-1, clone MMHAR-2) was used to block IFNAR2 subunit of the common IFN type I receptor and neutralize IFN-I signaling. Depending on the experimental conditions, cells were treated for up to 24 h before infection in up to 20 µg/mL of α-IFNAR2 antibody. After infection, α-IFNAR2 was again added to cells at up to 20 µg/mL. In longer experiments, fresh antibody was added to the well at half of the original concentration every 7 days.

IFN ELISA and multiplex assay

Were performed using the Human IFN Beta ELISA Kit, High Sensitivity Serum, Plasma, TCM (PBL Assay Science, USA, # 41415-1) and the LEGENDplex™ Human Anti-Virus Response Panel (BioLegend, USA, # 740390) according to manufacturer's instructions. Nominal limit of detection for ELISA was 0.39 U/mL (1.17 pg/mL).

Flow cytometric analysis of infection

Infected cells were DAPI stained before trypsinization for 1 min at 1:1000 PBS solution in 100 µL per well, thoroughly washed and trypsinized. 120 µL FACS buffer was added to each well, cells were thoroughly resuspended and analyzed with a BD LSRII SORP flow cytometer equipped with a HTS high throughput sampler.

Statistical analysis

Appropriate statistical analysis was carried out using GraphPad Prism software, based on the data and plot type as stated in figure legends. Where multiple conditions were compared to a control condition (**Fig. 1, 2, 6 & S3A**), analysis of variance (ANOVA) of group means was used as non-parametric (non-Gaussian distribution) test (Kruskal-Wallis) with multiple comparisons, against mean rank of the common control group (Dunn's test), or in grouped data (**Fig. 7**), against the control in that group (Dunnett's test). Where multiple conditions were tested against each other (**Fig. S4B**), ordinary one-way ANOVA with Holm-Sidak's multiple comparisons was sued. Where a single condition was compared to a single control (**Fig. 3C)**, unpaired non-parametric t-test (Mann Whitney) was used. Where a single condition was compared to a control within grouped data, two-way ANOVA with multiple comparisons of means (Sidak's test) (**Fig. 4C**) or Tukey's test were used (**Fig. 5C**). All conditions within the same group were compared using Bonferroni's multiple comparisons test (**Fig. S4C**).

Ethics statements

Non-parenchymal human liver cells were supplied by the Clinic for General, Abdominal and Transplant Surgery, Hannover Medical School (MHH) under the ethical permit number 2188-2014 from MHH ethics commission. Human lung tissue samples were supplied by the Department of Cardiothoracic, Transplantation and Vascular Surgery, MHH under the ethical permit number 7191 from MHH ethics commission. Leukoreduction system (LRS) chambers for PBMC isolation were supplied by the Institute for Transfusion Medicine, MHH under the ethical permit 2519-2014 from MHH ethics commission.

Acknowledgments

We would like to thank Christian Sinzger and Kerstin Laib Sampaio for generously providing us with the TB40/E-UL32-GFP/UL100-mCherry reporter virus and Harald Wodrich for providing us with primary human foreskin fibroblasts. In addition, we thank Julia Holzki and Zeeshan Chaudhry for ideas and discussion, Ayse Barut and Ilona Bretag for their help in preparation of donated PBMCs and primary cells, as well as Johannes Greiner for help in setting up some experiments. This work was supported by the German Scientific foundation (DFG) through the grant SFB900 TP-B2 and through the Infect-ERA grant eDEVILLI to LCS. The funding agency had no role in study design, data collection and interpretation, or in the decision to submit the work for publication.

References

1. **Boppana SB, Fowler KB.** 2007. Persistence in the population: epidemiology and transmisson. Persistence in the population: epidemiology and transmisson.
2. **Söderberg-Nauclér C, Nelson JA.** 1999. Human cytomegalovirus latency and reactivation–a delicate balance between the virus and its host's immune system. Intervirology.
3. **Sissons JGP, Bain M, Wills MR.** 2002. Latency and reactivation of human cytomegalovirus. The Journal of infection doi:10.1053/jinf.2001.0948.
4. **Legendre C, Pascual M.** 2008. Improving outcomes for solid-organ transplant recipients at risk from cytomegalovirus infection: late-onset disease and indirect consequences. Clin Infect Dis **46:**732-740.
5. **Sylwester AW, Mitchell BL, Edgar JB, Taormina C, Pelte C, Ruchti F, Sleath PR, Grabstein KH, Hosken NA, Kern F, Nelson JA, Picker LJ.** 2005. Broadly targeted human cytomegalovirus-specific CD4+ and CD8+ T cells dominate the memory compartments of exposed subjects. J Exp Med **202:**673-685.
6. **Lathbury LJ, Allan JE, Shellam GR, Scalzo AA.** 1996. Effect of host genotype in determining the relative roles of natural killer cells and T cells in mediating protection against murine cytomegalovirus infection. Journal of general virology **77:**2605-2613.
7. **Miletić A, Krmpotić A, Jonjić S.** 2013. The evolutionary arms race between NK cells and viruses: who gets the short end of the stick? European journal of immunology **43:**867-877.
8. **Collin M, McGovern N, Haniffa M.** 2013. Human dendritic cell subsets. Immunology doi:10.1111/imm.12117.
9. **Romani N, Gruner S, Brang D, Kämpgen E.** 1994. Proliferating dendritic cell progenitors in human blood. Journal of … doi:10.1084/jem.180.1.83.
10. **Jahn G, Stenglein S, Riegler S, Einsele H, Sinzger C.** 1999. Human cytomegalovirus infection of immature dendritic cells and macrophages. Intervirology **42:**365-372.
11. **Riegler S, Hebart H, Einsele H, Brossart P, Jahn G, Sinzger C.** 2000. Monocyte-derived dendritic cells are permissive to the complete replicative cycle of human cytomegalovirus. J Gen Virol **81:**393-399.
12. **Beck K, Meyer-König U, Weidmann M.** 2003. Human cytomegalovirus impairs dendritic cell function: a novel mechanism of human cytomegalovirus immune escape. European journal of … doi:10.1002/eji.200323612.
13. **Reeves MB, Sinclair JH.** 2013. Circulating dendritic cells isolated from healthy seropositive donors are sites of human cytomegalovirus reactivation in vivo. J Virol **87:**10660-10667.
14. **Renneson J, Dutta B, Goriely S, Danis B.** 2009. IL-12 and type I IFN response of neonatal myeloid DC to human CMV infection. European journal of … doi:10.1002/eji.200939414.
15. **Paijo J, Doring M, Spanier J, Grabski E, Nooruzzaman M, Schmidt T, Witte G, Messerle M, Hornung V, Kaever V, Kalinke U.** 2016. cGAS Senses Human Cytomegalovirus and Induces Type I Interferon Responses in Human Monocyte-Derived Cells. PLoS Pathog **12:**e1005546.
16. **Raftery MJ, Schwab M, Eibert SM, Samstag Y.** 2001. Targeting the function of mature dendritic cells by human cytomegalovirus: a multilayered viral defense strategy. Immunity.
17. **Jenkins C, Abendroth A, Slobedman B.** 2004. A novel viral transcript with homology to human interleukin-10 is expressed during latent human cytomegalovirus infection. J Virol **78:**1440-1447.
18. **Chang WLW, Barry PA, Szubin R, Wang D.** 2009. Human cytomegalovirus suppresses type I interferon secretion by plasmacytoid dendritic cells through its interleukin 10 homolog. Virology.
19. **Avdic S, McSharry BP, Slobedman B.** 2014. Modulation of dendritic cell functions by viral IL-10 encoded by human cytomegalovirus. Front Microbiol **5:**337.
20. **Alexandre YO, Cocita CD, Ghilas S, Dalod M.** 2014. Deciphering the role of DC subsets in MCMV infection to better understand immune protection against viral infections. Front Microbiol **5:**378.

21. **Benedict CA, Loewendorf A, Garcia Z.** 2008. Dendritic cell programming by cytomegalovirus stunts naive T cell responses via the PD-L1/PD-1 pathway. The Journal of … doi:10.4049/jimmunol.180.7.4836.
22. **Holzki J, Dağ F, Dekhtiarenko I, Rand U, Casalegno-Garduño R, Trittel S, May T, Riese P, Čičin-Šain L.** 2015. Type I Interferon Released by Myeloid Dendritic Cells Reversibly Impairs Cytomegalovirus Replication by Inhibiting Immediate Early Gene Expression. Journal of Virology **89**.
23. **Streblow DN, Varnum SM, Smith RD.** 2006. A proteomics analysis of human cytomegalovirus particles. … : molecular biology and ….
24. **Tang Q, Maul GG.** 2006. Mouse cytomegalovirus crosses the species barrier with help from a few human cytomegalovirus proteins. Journal of virology doi:10.1128/JVI.00684-06.
25. **Rawlinson WD, Farrell HE, Barrell BG.** 1996. Analysis of the complete DNA sequence of murine cytomegalovirus. Journal of virology **70:**8833-8849.
26. **Scheu S, Dresing P.** 2008. Visualization of IFNβ production by plasmacytoid versus conventional dendritic cells under specific stimulation conditions in vivo. Proceedings of the … doi:10.1073/pnas.0808537105.
27. **Puttur F, Francozo M, Solmaz G, Bueno C.** 2016. Conventional Dendritic Cells Confer Protection against Mouse Cytomegalovirus Infection via TLR9 and MyD88 Signaling. Cell reports.
28. **Döring M, Lessin I, Frenz T, Spanier J.** 2014. M27 expressed by cytomegalovirus counteracts effective type I interferon induction of myeloid cells but not of plasmacytoid dendritic cells. Journal of … doi:10.1128/JVI.00216-14.
29. **Tyznik AJ, Verma S, Wang Q.** 2014. Distinct requirements for activation of NKT and NK cells during viral infection. The Journal of … doi:10.4049/jimmunol.1300837.
30. **Banchereau J, Steinman RM.** 1998. Dendritic cells and the control of immunity. Nature **392:**245-252.
31. **Swiecki M, Gilfillan S, Vermi W, Wang Y, Colonna M.** 2010. Plasmacytoid dendritic cell ablation impacts early interferon responses and antiviral NK and CD8(+) T cell accrual. Immunity **33:**955-966.
32. **Nair S, Archer GE, Tedder TF.** 2001. Current Protocols in Immunology. Current Protocols in Immunology doi:10.1002/0471142735.im0732s99.
33. **Sampaio KL, Jahn G, Sinzger C.** 2013. Applications for a dual fluorescent human cytomegalovirus in the analysis of viral entry. Applications for a dual fluorescent human cytomegalovirus in the analysis of viral entry.
34. **Kodama A, Tanaka R, Saito M, Ansari AA, Tanaka Y.** 2013. A novel and simple method for generation of human dendritic cells from unfractionated peripheral blood mononuclear cells within 2 days: its application for induction of HIV-1-reactive CD4(+) T cells in the hu-PBL SCID mice. Frontiers in microbiology **4:**292.
35. **Shaner NC, Lambert GG, Chammas A, Ni Y, Cranfill PJ, Baird MA, Sell BR, Allen JR, Day RN, Israelsson M, Davidson MW, Wang J.** 2013. A bright monomeric green fluorescent protein derived from Branchiostoma lanceolatum. Nature methods **10:**407-409.
36. **Osborn JE, Walker DL.** 1968. Enhancement of infectivity of murine cytomegalovirus in vitro by centrifugal inoculation. J Virol **2:**853-858.
37. **Doring M, Lessin I, Frenz T, Spanier J, Kessler A, Tegtmeyer P, Dag F, Thiel N, Trilling M, Lienenklaus S, Weiss S, Scheu S, Messerle M, Cicin-Sain L, Hengel H, Kalinke U.** 2014. M27 expressed by cytomegalovirus counteracts effective type I interferon induction of myeloid cells but not of plasmacytoid dendritic cells. J Virol **88:**13638-13650.
38. **Pascutti MF, Rodriguez AM, Falivene J, Giavedoni L, Drexler I, Gherardi MM.** 2011. Interplay between modified vaccinia virus Ankara and dendritic cells: phenotypic and functional maturation of bystander dendritic cells. J Virol **85:**5532-5545.

39. **Domanski P, Witte M, Kellum M, Rubinstein M, Hackett R, Pitha P, Colamonici OR.** 1995. Cloning and expression of a long form of the subunit of the interferon receptor that is required for signaling. Journal of Biological Chemistry **270:**21606-21611.
40. **Stegmann C, Hochdorfer D, Lieber D, Subramanian N, Stohr D, Laib Sampaio K, Sinzger C.** 2017. A derivative of platelet-derived growth factor receptor alpha binds to the trimer of human cytomegalovirus and inhibits entry into fibroblasts and endothelial cells. PLoS Pathog **13:**e1006273.
41. **Xiaofei E, Stadler BM, Debatis M, Wang S, Lu S, Kowalik TF.** 2012. RNA interference-mediated targeting of human cytomegalovirus immediate-early or early gene products inhibits viral replication with differential effects on cellular functions. J Virol **86:**5660-5673.
42. **Hahn G, Jores R, Mocarski ES.** 1998. Cytomegalovirus remains latent in a common precursor of dendritic and myeloid cells. Proceedings of the National Academy of Sciences **95:**3937-3942.
43. **Reeves MB, Lehner PJ.** 2005. An in vitro model for the regulation of human cytomegalovirus latency and reactivation in dendritic cells by chromatin remodelling. Journal of General ….
44. **Scheu S, Dresing P, Locksley RM.** 2008. Visualization of IFNbeta production by plasmacytoid versus conventional dendritic cells under specific stimulation conditions in vivo. Proc Natl Acad Sci U S A **105:**20416-20421.
45. **Jackson SE, Sedikides GX, Mason GM, Okecha G, Wills MR.** 2017. Human Cytomegalovirus (HCMV)-Specific CD4+ T Cells Are Polyfunctional and Can Respond to HCMV-Infected Dendritic Cells In Vitro. Journal of Virology **91**.
46. **Goodrum F, Reeves M, Sinclair J, High K, Shenk T.** 2007. Human cytomegalovirus sequences expressed in latently infected individuals promote a latent infection in vitro. Blood **110:**937-945.
47. **Cheung AK, Abendroth A, Cunningham AL, Slobedman B.** 2006. Viral gene expression during the establishment of human cytomegalovirus latent infection in myeloid progenitor cells. Blood **108:**3691-3699.
48. **Buehler J, Zeltzer S, Reitsma J, Petrucelli A, Umashankar M, Rak M, Zagallo P, Schroeder J, Terhune S, Goodrum F.** 2016. Opposing Regulation of the EGF Receptor: A Molecular Switch Controlling Cytomegalovirus Latency and Replication. PLoS Pathog **12:**e1005655.
49. **Reeves MB, Compton T.** 2011. Inhibition of inflammatory interleukin-6 activity via extracellular signal-regulated kinase-mitogen-activated protein kinase signaling antagonizes human cytomegalovirus reactivation from dendritic cells. J Virol **85:**12750-12758.
50. **van Beijnum JR, Rousch M, Castermans K, van der Linden E, Griffioen AW.** 2008. Isolation of endothelial cells from fresh tissues. Nat Protoc **3:**1085-1091.
51. **Fujino N, Kubo H, Ota C, Suzuki T, Suzuki S, Yamada M, Takahashi T, He M, Suzuki T, Kondo T, Yamaya M.** 2012. A novel method for isolating individual cellular components from the adult human distal lung. Am J Respir Cell Mol Biol **46:**422-430.
52. **Dietz AB, Bulur PA, Emery RL, Winters JL, Epps DE, Zubair AC, Vuk-Pavlović S.** 2006. A novel source of viable peripheral blood mononuclear cells from leukoreduction system chambers. Transfusion **46:**2083-2089.
53. **Fuss IJ, Kanof ME, Smith PD, Zola H.** 2009. Current Protocols in Immunology. wiley doi:10.1002/0471142735.im0701s85.
54. **Wahl LM, Wahl SM, Smythies LE, Smith PD.** 2001. Current Protocols in Immunology. Current Protocols in Immunology doi:10.1002/0471142735.im0706as70.
55. **Obermaier B, Dauer M, Herten J, Schad K, Endres S, Eigler A.** 2003. Development of a new protocol for 2-day generation of mature dendritic cells from human monocytes. Biological procedures online **5:**197-203.
56. **Dauer M, Obermaier B, Herten J, Haerle C, Pohl K, Rothenfusser S, Schnurr M, Endres S, Eigler A.** 2003. Mature dendritic cells derived from human monocytes within 48 hours: a novel strategy for dendritic cell differentiation from blood precursors. J Immunol **170:**4069-4076.

57. **Tischer BK, Smith GA, Osterrieder N.** 2010. En passant mutagenesis: a two step markerless red recombination system. Methods in molecular biology (Clifton, NJ) **634:**421-430.

58. **Sinzger C, Hahn G, Digel M.** 2008. Cloning and sequencing of a highly productive, endotheliotropic virus strain derived from human cytomegalovirus TB40/E. Cloning and sequencing of a highly productive, endotheliotropic virus strain derived from human cytomegalovirus TB40/E.

59. **Kim JH, Lee S-RR, Li L-HH, Park H-JJ, Park J-HH, Lee KY, Kim M-KK, Shin BA, Choi S-YY.** 2011. High cleavage efficiency of a 2A peptide derived from porcine teschovirus-1 in human cell lines, zebrafish and mice. PloS one **6**.

60. **Schindelin J, Arganda-Carreras I, Frise E, Kaynig V, Longair M, Pietzsch T, Preibisch S, Rueden C, Saalfeld S, Schmid B, Tinevez JY, White DJ, Hartenstein V, Eliceiri K, Tomancak P, Cardona A.** 2012. Fiji: an open-source platform for biological-image analysis. Nat Methods **9:**676-682.

Figure Legends

Figure 1: mo-DCs suppress spread of late dual reporter HCMV^{dLr} in coculture with infected human MRC-5 fibroblasts.

Human mo-DCs were cocultured at indicated E:T ratios with MRC-5 cells infected with HCMV^{dLr} infected with 375 PFU of HCMV^{IEr} (MOI 0.0125). Mo-DC were added immediately upon removal of the virus. Number of GFP/mCherry expressing cells at 5-6 days post infection in co-culture with (A) conventionally generated, or (B) rapidly generated mo-DCs are shown. Dot plots depict combined data from at least three independent experiments with mo-DCs generated from 6 (A), or 17 (B) PBMC donors. Horizontal lines denote group means, and error bars the standard deviation. (C) Co-cultures of infected MRC-5 and mo-DC at indicated E:T ratios in 6-well replicates were infected with 1050 PFU of HCMV^{IEr} (MOI 0.035). Virus titer in SN at dpi 6 was established by plaque assay. Symbols indicate individual replicates, bars are mean values. Each group was statistically analyzed by non-parametric two-way ANOVA (Kruskal–Wallis) with Dunn's multiple comparisons test against the control (w/o mo-DC) group, * = $p < 0.05$, *** = $p<0.001$ and **** = $p<0.0001$. (D) GFP/mCherry expressing cells were quantified in MRC-5 infected with 45 PFU (MOI 0.0015) of HCMV^{dLr} in the presence of mo-DCs at 6, 9, 12 and 15 dpi (blue squares) and compared to controls infected in absence of mo-DC (black circles), or those where mo-DCs were removed at dpi 6. Plotted are combined data from 2 independent experiments, mean with SD. (E) Cells were infected as in (D), but only 6 PFU per well (MOI 0.0002) were added to MRC-5 in 12-well replicates. Well was reported as positive if ≥ 1 fluorescent cell was observed. Plot depicts combined data from four independent experiments.

Figure 2: mo-DCs suppress spread of immediate early reporter HCMV^{IEr} in coculture with infected human fibroblasts.

706 Mo-DCs were cocultured at increasing E:T ratios with HCMV^{IEr} infected MRC-5 at (A) 150
707 PFU/well (MOI 0.005). mNeonGreen expressing infection foci were manually quantified in
708 each well at 2-3 dpi. Dot plot depicts combined data from four independent experiments
709 with mo-DCs generated from five donors, depicted are means with standard deviation.
710 Kruskal–Wallis one-way ANOVA with Dunn's multiple comparisons test for each data set
711 against the control data set (without mo-DCs) was used, *** = p<0.001, **** = p<0.0001. (B)
712 Representative images from cocultures infected with MOI 0.035 (1050 PFU/well) at 8 and (C)
713 23 dpi. (D) As in **Figure 1E**, 6 PFU/well (MOI 0.0002) of HCMV^{IEr} was added to MRC-5 in 12-
714 well replicates. Well was reported as positive if ≥ 1 fluorescent cell was observed. Plot
715 depicts combined data from five independent experiments (n=2 for day 21).

716 **Figure 3: The antiviral factors from mo-DCs delay the onset and repress the HCMV IE gene**
717 **expression in fibroblasts**

718 MRC-5 fibroblasts were infected with HCMV^{IEr} at MOI of 0.035 using centrifugal
719 enhancement, medium (blue line), or the antiviral supernatant (from coculture of infected
720 MRC-5 and mo-DCs, referred to as SN°) (red line), was immediately added to them and
721 infection was followed by epifluorescence time lapse imaging in 24 fields per condition at
722 the rate of one frame per 20 min. (A) Solid lines show 3-point smoothing of average signal
723 ratio (signal from infected cells to background signal of the field) from 24-fields, with SD of
724 average up to 35 hours post infection (pi). Representative plot from one out of three
725 independent experiments. (B) Signal ratio in untreated cells deviated from baseline signal
726 ratio (dashed line) at around 3 hpi (blue arrow) while this was at >5 hours for SN° treated
727 cells (red arrow). (C) Scatter dot plots shows distribution of signal onset in each field of
728 untreated (blue) and SN° treated (red) condition. Unpaired non-parametric t-test (Mann
729 Whitney test) was used, **** = p < 0.0001. (D) Representative time series image montages

730 from (A) up to 174 house pi. ie1/2 associated mNeonGreen signal in GFP channel is depicted
731 in false colors (Fire Blue Green Look Up Table, LUT) for better visibility. Scale bars are 100
732 µm.

733 **Figure 4: Blocking interferon α/β receptor increases IFN-β availability in coculture media,**
734 **yet does not negatively affect the antiviral function of mo-DCs**

735 (A) IFN-β concentration was measured by ELISA in coculture SNs from MRC-5 infected with
736 1050 PFUs of HCMV^{IEr} (MOI 0.035) and cocultured with or without mo-DCs in presence or
737 absence of 10 µg/mL α-IFNAR2 for 14 days. Bars are representative from one out of two
738 independent experiments. (B) Infectious virus titers were measured in SNs from (A).
739 Representative data from one out of three independent experiments show mean with SD.
740 (C) MRC-5 in 8-well replicates were infected with 150 PFU (MOI 0.005) of HCMV^{IEr} and
741 cocultured with mo-DCs in presence or absence of 10 µg/mL α-IFNAR2 and number of
742 infection foci was quantified at 3 dpi. Data from one out of three independent experiments
743 showing mean with SD. Two-way ANOVA repeated-measures with Sidak's multiple
744 comparisons test was used, ns= $p \geq 0.05$, ** = $p < 0.01$. (D) Representative images from (C) at 8
745 dpi.

746 **Figure 5: Pretreatment with the antiviral SN improves control of infection**

747 (A) Antiviral SN° from two donors (H.BS#22 & #23) were added to MRC-5 24 h before
748 infection and then replaced with medium 21 h later (pre-treatment, white bars).
749 Synchronized infection of cells with HCMV^{IEr} at MOI 0.035 in medium or SN° (added at
750 infection, gray bars) was carried out and SN° was added to all conditions after removing the
751 virus (post-treatment, black bars). (B) Gating strategy for flow cytometric analysis. (C) Bars
752 show the percentage of infected cells in four replicates and (D) the mean fluorescence

753 intensity of the infected cells for each condition. Regular two-way ANOVA with Tukey's
754 multiple comparisons between all data sets was used in one representative out of two
755 independent experiments with *** = p <0.001, **** = p<0.0001.

756 **Figure 6: mo-DC contact with infected MRC-5 cells is required for stimulation of mo-DC**
757 **antiviral function and does not involve IFN**

758 (A) Representative images at 5 dpi and (B) quantification at 5-6 dpi of spread of infection
759 $HCMV^{dLr}$ (MOI 0.0125) in MRC-5 treated with, from left to right, culture medium as control,
760 SN of E:T 10:1 mo-DC/MRC-5 coculture infected with $HCMV^{dLr}$ (MOI 0.001), or uninfected, or
761 SN of $1x10^6$ mo-DCs infected at MOI of 1 collected at 6-8 dpi (experimental design depicted
762 in **Fig. S1B**). Combined data from at least three independent experiments with mo-DCs
763 generated from 6 different PBMC donors, showing mean with SD. (C) Representative images
764 at 8 dpi and (D) quantification at 3 dpi of the spread of $HCMV^{IEr}$ (MOI 0.005) infection treated
765 as in (B). (E) Concentration of IFN-α2, -β, -γ, -λ1 and λ2/3 were measured in the SNs using a
766 multi-analyte flow assay (LEGENDplex), with n ≥ 9 samples for antiviral SN and n ≥ 3 for other
767 conditions not differences were statistically significant. Kruskal-Wallis ANOVA with Dunn's
768 multiple comparison test for each column against the control column (culture medium) was
769 used, ns= p≥0.05, **** = p<0.0001.

770 **Figure 7: mo-DCs coculture and their coculture supernatants suppress HCMV spread in**
771 **primary human cells**

772 Primary human cells were infected with 300 PFU (MOI 0.01) and (A) cocultured with mo-DCs,
773 or (B) SNs were added to them and the spread of infection was quantified at 5 dpi (as in Fig.
774 6). Combined data from two independent experiments showing mean with SD. Two-way

775 ANOVA with Dunnett's multiple comparison test, ns= p≥0.05, * = p<0.05, *** = p<0.001,

776 **** = p<0.0001.

Figure 1

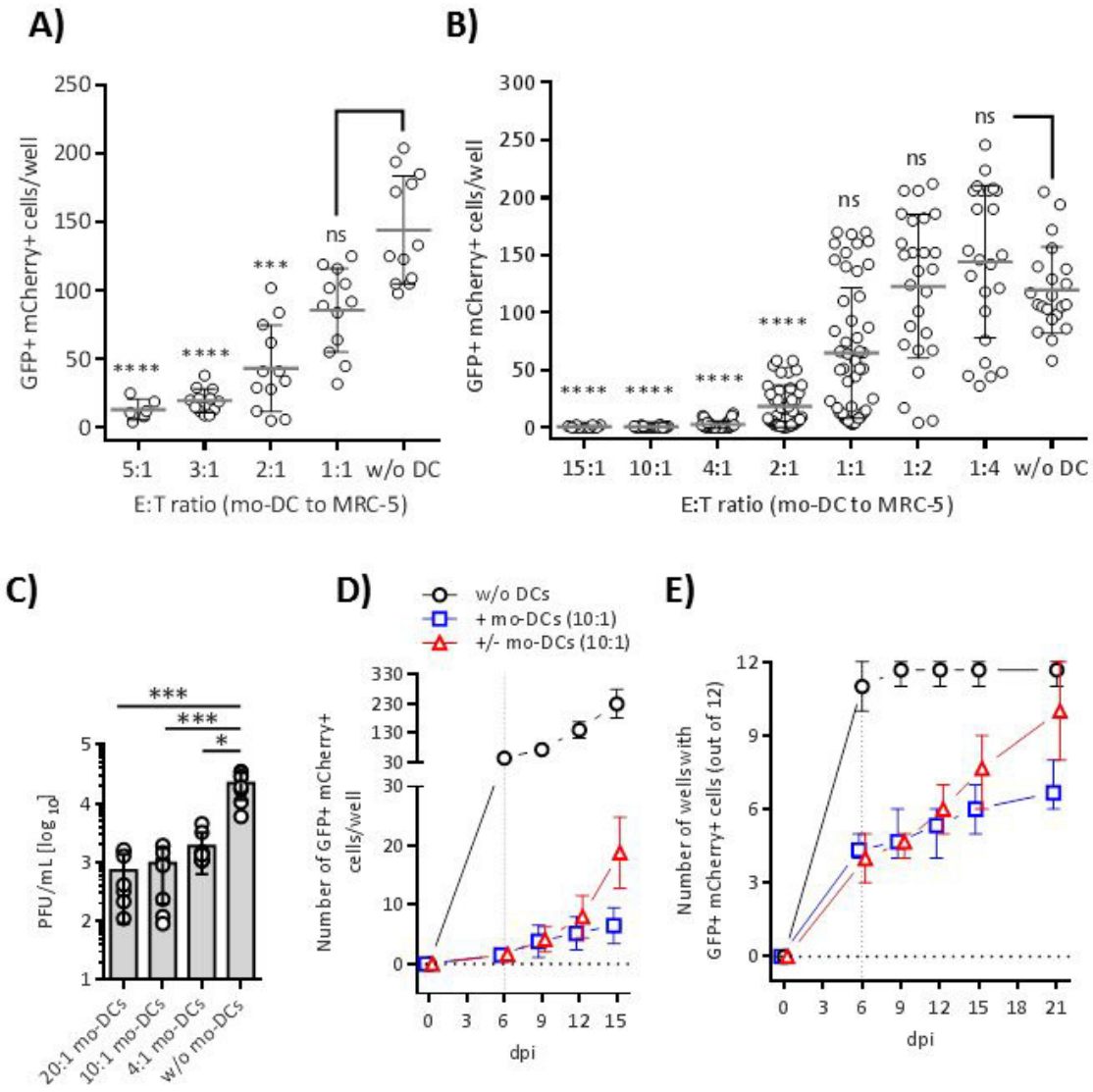

Figure 2

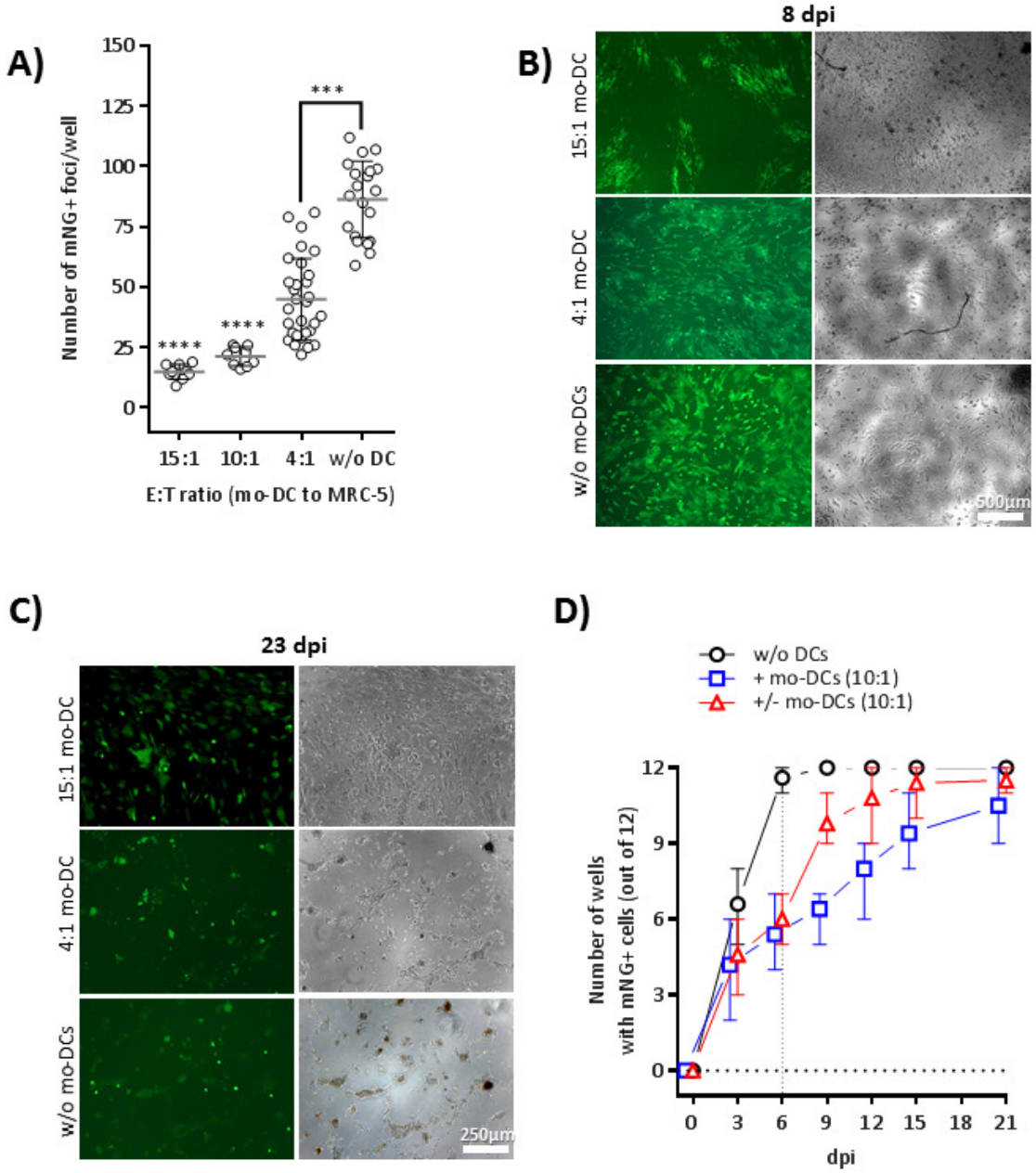

Figure 3

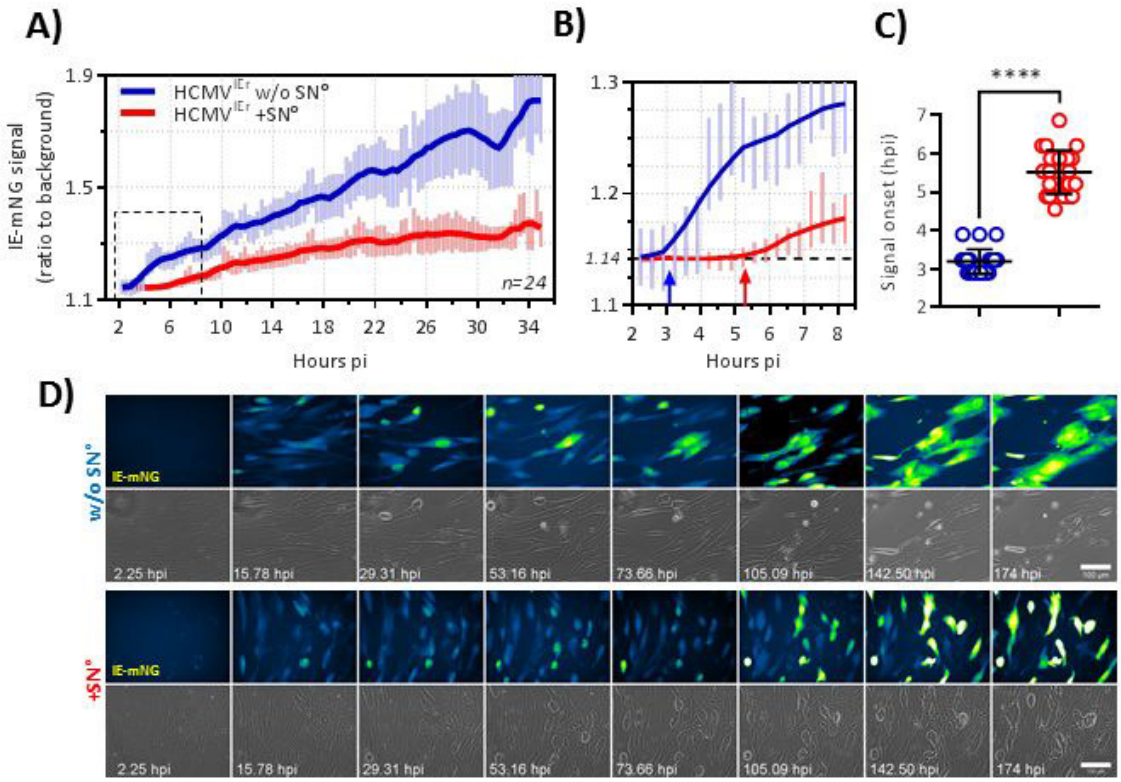

Figure 4

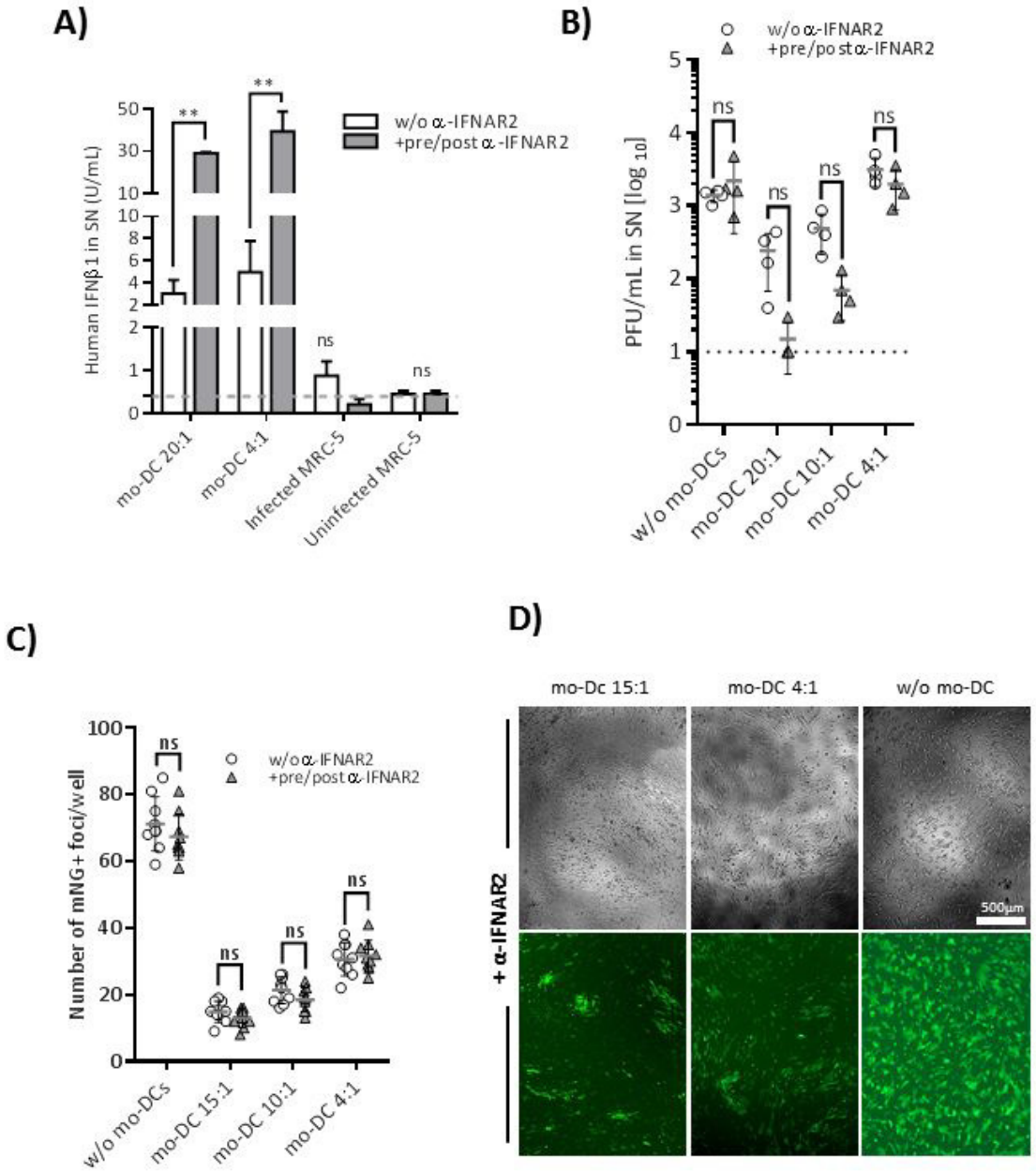

Figure 5

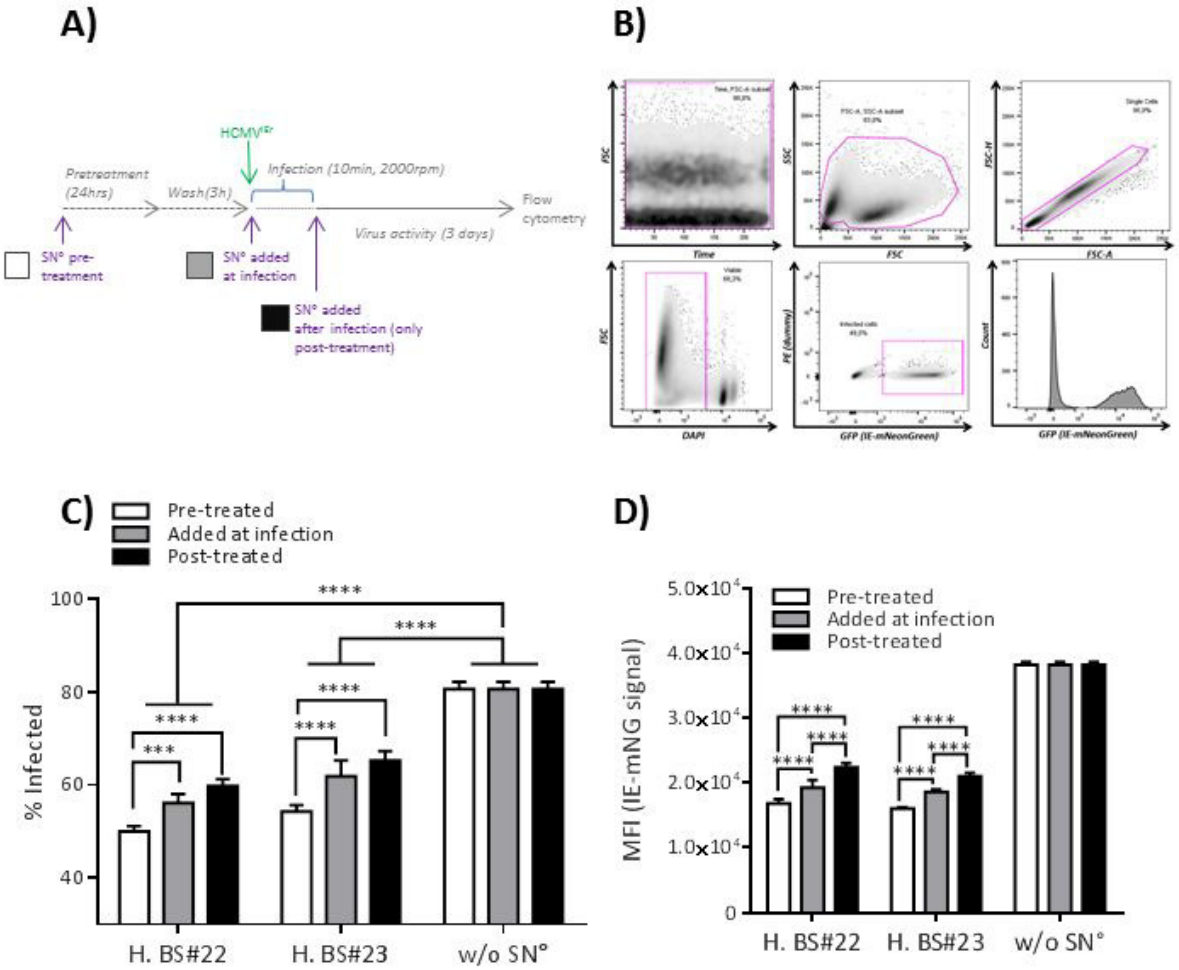

Figure 6

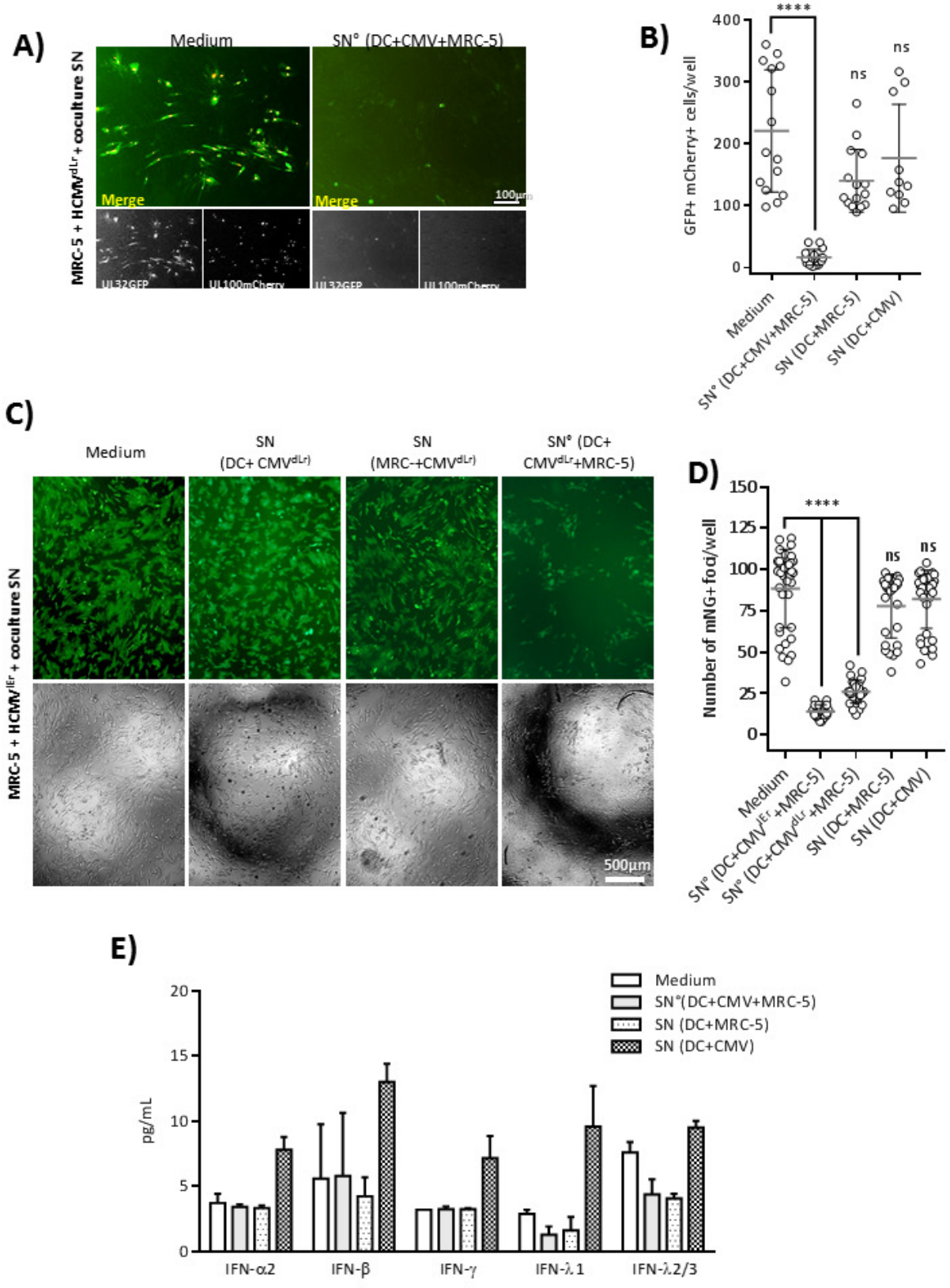

Figure 7